Available online at www.sciencedirect.com
ScienceDirect
Mathematical and Computer Modelling 47 (2008) 1134–1149
MATHEMATICAL AND COMPUTER MODELLING
www.elsevier.com/locate/mcm

Parameter uncertainty, sensitivity analysis and prediction error in a water-balance hydrological model

Kurt K. Benke[a,*], Kim E. Lowell[a,b], Andrew J. Hamilton[a,c]

[a] *Primary Industries Research Victoria – Parkville Centre, Department of Primary Industries, PO Box 4166, Parkville, Victoria 3052, Australia*
[b] *CRC for Spatial Information, The University of Melbourne, 723 Swanston Street, Ground floor, Carlton, Victoria 3052, Australia*
[c] *School of Resource Management, Faculty of Land and Food Resources, The University of Melbourne, 500 Yarra Boulevard, Richmond, Victoria 3121, Australia*

Received 20 April 2007; accepted 16 May 2007

Abstract

Analysis of uncertainty is often neglected in the evaluation of complex systems models, such as computational models used in hydrology or ecology. Prediction uncertainty arises from a variety of sources, such as input error, calibration accuracy, parameter sensitivity and parameter uncertainty. In this study, various computational approaches were investigated for analysing the impact of parameter uncertainty on predictions of streamflow for a water-balance hydrological model used in eastern Australia. The parameters and associated equations which had greatest impact on model output were determined by combining differential error analysis and Monte Carlo simulation with stochastic and deterministic sensitivity analysis. This integrated approach aids in the identification of insignificant or redundant parameters and provides support for further simplifications in the mathematical structure underlying the model. Parameter uncertainty was represented by a probability distribution and simulation experiments revealed that the shape (skewness) of the distribution had a significant effect on model output uncertainty. More specifically, increasing negative skewness of the parameter distribution correlated with decreasing width of the model output confidence interval (i.e. resulting in less uncertainty). For skewed distributions, characterisation of uncertainty is more accurate using the confidence interval from the cumulative distribution rather than using variance. The analytic approach also identified the key parameters and the non-linear flux equation most influential in affecting model output uncertainty.

Keywords: Complex systems; Error propagation; Hydrological model; Monte Carlo simulation; Risk; Sensitivity analysis; Uncertainty; 2C; 2CSalt

1. Introduction

Hydrological models have been widely used in the past to provide catchment management with information on the interaction of water, energy and vegetation processes distributed over space and time [1]. Computational models can be used to quantify surface and groundwater contributions to streamflow and salt export at catchment scale, and have particular importance with respect to the effect of changes in land-use. For example, the impact of land-usage on salt and water yield would require the evaluation of tree-planting strategies, the consequent effect on bio-diversity, and

* Corresponding author.
E-mail address: kurt.benke@dpi.vic.gov.au (K.K. Benke).

0895-7177/$ - see front matter © 2007 Elsevier Ltd. All rights reserved.
doi:10.1016/j.mcm.2007.05.017

optimisation of land-use with respect to impact on stream salinity. In particular, an imbalance in the proportion of land devoted to urban, farming and forestry planning could dramatically reduce water available to streamflow and storage in a catchment.

A typical hydrological model consists of a large number of coupled equations describing the direction of water flow, including surface and sub-surface flows, providing predictions of monthly and annual streamflow or salt deposition. Additional inputs represent the spatial mosaic of climate, soil type, topography and land use [2]. Temporal inputs include estimates of surface runoff, sub-surface lateral flow, recharge, and potential evaporation. The computational procedure may estimate the partitioning between surface, lateral and groundwater pathways in the catchment and be applied over daily, monthly or yearly increments.

Historically, most hydrological models have been deterministic in that model parameters and inputs are represented by single values or point estimates — e.g. 2C or 2CSalt [3], BC2C [4] and other coupled salt and water-balance models [5]. More recently, reviews have been published on the role of calibration and uncertainty in the modelling process [1,6]. With respect to the specific aim of calibration and parameter estimation, uncertainty has been addressed by proposing various regression and probabilistic approaches, such as Generalised Likelihood Uncertainty Estimation (GLUE) [7], Markov Chain Monte Carlo (MCMC) [8], and also MCMC/Bayesian inference approaches, such as MCMC Global Sensitivity Analysis (MCMC-GSA) [9] and Bayesian Approach to Total Error Analysis (BATEA) [10,11].

In general, hydrological models incorporate many parameters (some statistical and some with physical significance), most of which require measurements from resource-intensive field exercises which are used to calibrate the model by statistical methods, such as least-squares regression analysis or the approaches cited in the previous paragraph. In some cases, parameters with physical significance may be adjusted interactively during calibration. Irrespective of the method used for parameter estimation, one often has little sense of which parameters have the most influence on model output. Indeed, some parameters may have such little impact that they could be easily ignored, leading to simplification of the mathematical structure of the model. A primary concern in this study was to explore the sensitivity of predictions to parameter variability in order to establish their relative importance for accurate calibration.

By including uncertainty in model parameters, rather than using point estimates, more information is available to the catchment manager with respect to prediction error. In a fundamental sense, uncertainty associated with model output may be represented as a probability distribution or as a specific statistical quantity, such as the 95th percentile result from the cumulative probability distribution (i.e. what is the annual streamflow prediction with a 95% probability?). By introducing notions of confidence and probability, this approach provides more information than a single point estimate and informs policy developers about the degree of risk associated with particular actions (Fig. 1).

Kuczera and Parent [8] studied MCMC/Bayesian approaches to calibration uncertainty and reported a case study for the CATPRO salinity model. During calibration, they observed a bimodal histogram for one parameter, which they attributed to non-stationarity in the time-series input data. In general, however, there has been very little work reported on the shape of parameter distributions and the effect on prediction uncertainty. One objective of the current investigation was to examine the effect of parameter uncertainty on prediction uncertainty in a prototypical hydrological model (a water-balance model), where the parameters have already been assigned. The fixed parameters were subjected to systematic and random perturbations and the effect observed at the model output. The parameters were represented by distributions and the effect on prediction error and uncertainty explored by changing shape (skewness) under a variety of conditions using Monte Carlo simulation.

Another aim of the study was to present catchment managers and field hydrologists with straightforward computational strategies for the assessment of prediction uncertainty in a hydrological model. As a decision aid, this would benefit in the estimation of error, precision and confidence in the model predictions. In particular, isolation of those parameters with most effect on output would support the design and calibration of field experiments (noting cost reductions possible due to avoiding unnecessary measurement and excessive computational complexity). Whilst these investigations were carried out on the 2C hydrological model (a variant of the 2CSalt model), insights into how to deal with uncertainty are applicable to models of similar structure [3–5]. More specific aims of the investigation were (i) to investigate the transfer of uncertainty from designated key parameters to the model output by means of appropriate metrics, (ii) to examine the influence of the shape (skewness) in the parameter distributions on prediction error, and (iii) to conduct sensitivity analysis using both point estimates and parameter distributions.

2. Methods and software

2.1. The 2C model

The 2C test model [2,3] is mathematically well-defined, with a record of practical application in eastern Australia and has been rigorously tested. The recent extension of 2C to 2CSalt, whilst essentially the same model, has incorporated thresholds in the flux equations rather than as separate constraints, and the effectiveness of this change is currently under investigation. Aside from a test of various uncertainty metrics, the experimental results would be expected to reveal indicative behaviour for more general water-balance hydrological models with similar structure and, more important the methodology would be applicable to similar models [3–5].

The 2CSalt extension of the 2C model has been used to determine the effect of different land-use practices on predicted streamflow and salt load. Development commenced under the auspices of the Australian Cooperative Research Centre for Catchment Hydrology (CRC-CH), which has now been superseded by the eWater CRC. Model development is continuing for eventual use by State Agencies in order to provide a consistent output for reporting as part of catchment planning activities for State, Murray-Darling Basin and National Investment activities. The ongoing project is based on collaborative links with Industry Partners and CSIRO aimed at sharing modelling capability and information [3,4]. The 2CSalt model is also referenced by the Catchment Analysis Tool (CAT) developed by the Department of Primary Industries at Rutherglen in Victoria. CAT is a software interface and toolbox for the assessment of the impact of land-use on both paddock and catchment scale processes, such as surface runoff, sediment loss, nitrogen mobilisation, biomass yields, stream quality, and groundwater discharge [2].

The 2C model is a basic water-balance model characterised by a set of spatially distributed water processes with flux equations, thresholds and non-linearities [3]. The model produces outputs based on input data and parameters calibrated for a particular catchment and computes the direction of water flow, including surface and sub-surface flows. Model outputs include monthly time steps for runoff, lateral flow, recharge, discharge, evaporation and baseflow. The output of interest in this study is annual streamflow (obtained from integration of monthly time steps for streamflow). Annual streamflow was chosen as the performance index in order to avoid possible seasonal effects and to reduce the much greater computational burden and complexity of using 12-month time-series data as the output. The main aim of the study was to study the effectiveness of the uncertainty modelling approaches rather than the underlying hydrology of the application. The structure of the model and the relevant equations for calculating streamflow are presented in the Appendix.

In brief, streamflow is determined as a function of three stores: an unsaturated zone store, a hillslope aquifer store, and an alluvial mixing store. Spatial and temporal inputs are both required as input data (Fig. 2). The model features two types of spatial units within the catchment. A Groundwater Response Unit (GRU) represents an area defined by hydrogeological characteristics. The Hydrological Response Units (HRUs) represent the spatial mosaic of climate, soil type, topography and land use. Temporal inputs include estimates of surface runoff, sub-surface lateral flow, recharge, and potential evaporation. The model is implemented at the functional scale of the GRU, which is derived from the Digital Elevation Map (DEM). The standard output is a monthly time series for each defined Groundwater Response Unit (GRU), and from these outputs, additional information can be obtained for computation of annual streamflow and its components.

The 2C model was originally provided as Fortran 90 source code (re: Craig Beverly of DPI Rutherglen) and converted by the authors into Visual Basic source code for implementation as a VBA macro in Microsoft Excel. Risk analysis and uncertainty modelling were carried out using the Excel add-in @RISK (Palisade Corporation). The mathematical structure of the 2C hydrological model is outlined in the Appendix.

2.2. Computational experiments

Five parameters were chosen for investigation, based on past experience and observed sensitivity by model users and catchment analysts located at Rutherglen, Victoria: β_2 (shape parameter for storage/discharge for the aquifer store), β_3 (shape parameter for storage/discharge for the alluvial mixing store), ω (shape parameter for evaporation from the alluvial mixing store), $HQ_{\max}$ (maximum discharge from hillslope aquifer store), and $AQ_{\max}$ (maximum discharge from alluvial mixing store). The equations in which these parameters appear in the 2C model are documented in the Appendix. Initial conditions for experiments (definitions in the Appendix) were Area $= 2000\ \mathrm{m}^2$,

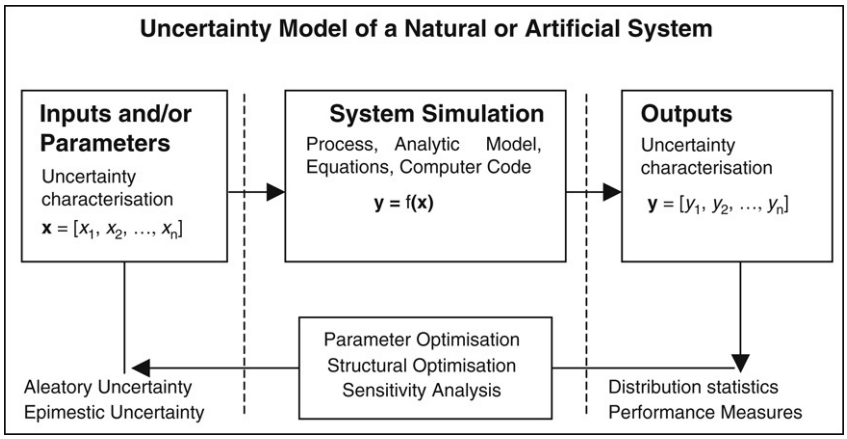

Fig. 1. Uncertainty in a complex system.

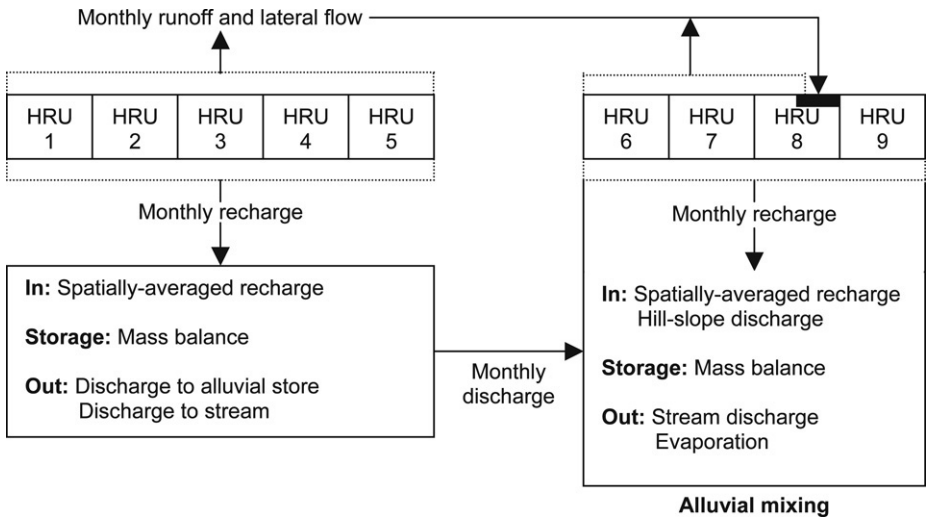

Fig. 2. Flow of water within a Ground Response Unit (GRU), adaptation from [3].

$\text{Area}_{\text{GRU}} = 4000\ \text{m}^2$, $HS_{\max} = 25{,}000\ \text{m}^3$, $HS_1 = 10{,}000\ \text{m}^3$, $AS_{\max} = 50{,}000\ \text{m}^3$, and $AS_1 = 20{,}000\ \text{m}^3$. The baseline test data and initial parameter values used for modelling uncertainty and sensitivity were consistent with the Bet Bet catchment in northern Victoria (see Fig. 3 and Section 2.3), to which 2C had previously been applied. More recent calibration studies have also been published [2]. For the predictive model, the time-series model output of monthly results was integrated to produce the annual streamflow prediction (to avoid seasonal variation).

Uncertainty, or variability, associated with the parameters was accounted for by representing each with a probability distribution. Specifically, the PERT distribution was used for reasons given below. The PERT distribution is a special case of the Beta distribution, and is specified by assigning minimum, maximum and most likely values, ($x_{\min}$, $x_{\max}$, x_{mode}) to the probability density function. The mean value is then calculated as follows,

$$x_{\text{mean}} = \frac{(x_{\min} + \lambda x_{\text{mode}} + x_{\max})}{(\lambda + 2)}, \tag{1}$$

where the scale parameter for the height of the distribution has default value $\lambda = 4$ [12,13]. This mean value is then used to compute the shape parameters, v and w, which are used in turn to sample the Beta distribution,

$$v = \frac{(x_{\text{mean}} - x_{\min})(2x_{\text{mode}} - x_{\min} - x_{\max})}{(x_{\text{mode}} - x_{\text{mean}})(x_{\max} - x_{\min})} \tag{2}$$

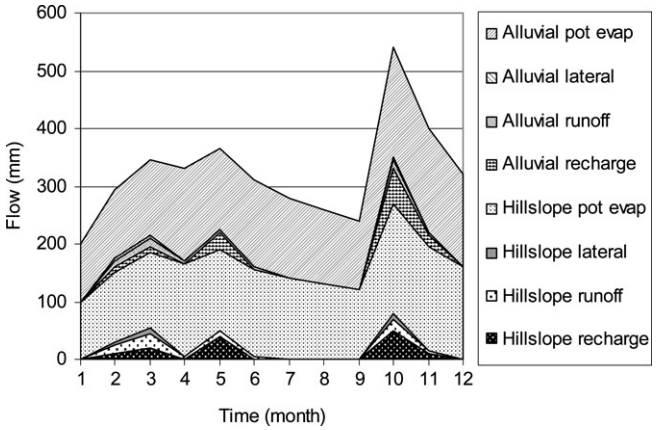

Fig. 3. Pre-processed spatial data showing alluvial and hillslope flows resolved into component contributions.

$$w = \frac{v(x_{\max} - x_{\text{mean}})}{(x_{\text{mean}} - x_{\min})}. \tag{3}$$

The probability density function for the Beta distribution is given by [13,14],

$$f(x) = \begin{cases} \dfrac{x^{v-1}(1-x)^{w-1}}{B(v,w)} & 0 \le x \le 1;\ v, w > 0 \\ 0 & \text{otherwise,} \end{cases} \tag{4}$$

where the standard Beta Function is given by

$$B(v,w) = \int_0^1 t^{v-1}(1-t)^{w-1}\mathrm{d}t. \tag{5}$$

The PERT distribution has a number of useful features when used as a sampling distribution in Monte Carlo simulation. First, it can be readily changed, in a controlled manner, from a distribution that is symmetric to one which is highly skewed, by varying a single parameter (the mode) appropriately, while keeping the interval width constant (*cf* other distributions which have infinite tails). Second, it can be used to provide a close fit to the normal or lognormal distributions, when this is required. Third, the finite bounds can be modified systematically by translation or dilation, with or without skew, to explore the consequent effects on the model output.

In the analysis reported here, the PERT distribution is used initially as a symmetric distribution to simulate a (normal) distribution. It is then adjusted systematically so as to investigate the effect of both *width* and *skewness* of the parameter distributions on the variance and uncertainty in the hydrological model predictions. Although not considered in this study, empirical parameter distributions may be investigated by sampling and collating historical parameter point estimates or using calibration data from the distribution of residuals arising from iterative non-linear regression analysis. Bayesian inference methods have also been used to estimate parameter distributions (by using Bayes Law and Markov Chain Monte Carlo simulation [8]).

2.3. Influence of parameter uncertainty on output uncertainty

The influence of parameter uncertainty on output uncertainty was studied through a series of forced perturbations on the parameters. The five parameters of interest were replaced with symmetrical PERT distributions and, in five consecutive Monte Carlo simulation experiments, the widths (ranges) of the probability distributions were increased jointly and incrementally. This involved increasing the tolerance on the mean (mode) values by ±20%, ±40%, ±60%, ±80% and ±100% (equivalent to coefficients of variation (CV) of 7.6%, 15.1%, 22.7%, 30.2%, 37.8%, respectively). The maximum tolerance was subject to the constraints $\beta_2, \beta_3, \omega, > 0$, as required by the flux equations described in the Appendix. The designated base values for the five-parameter set, β_2, β_3, ω, $HQ_{\max}$ and $AQ_{\max}$, prior to perturbation and simulation, were the elements of the parameter vector $\mathbf{x}_0 = [1, 1, 2, 20, 10]$ (which were typical of past calibration values, see also [2]).

Output uncertainty was represented by variance (σ^2) and the 90% confidence interval (90% CI). It is important to note that the 90% CI defined here is the difference between the 5th and 95th percentile values under the cumulative distribution curve of the output (*cf* the normal method of calculating a CI, which requires variance and assumes a symmetrical probability density function). A disadvantage of the variance-based approach is that, for a very skewed distribution, computed variance may fail to adequately characterise a long sweeping tail [15]. Both variance and 90% CI were evaluated in selected experiments for comparison. The gain factor, G, is the ratio of the output CV to input (or parameter) CV, and was used as a scale-free measure of amplification or attenuation in the perturbation transferred between parameter and model output.

2.4. Influence of skewness of parameters on skewness of outputs

The relationship between skewness of the parameter distribution and uncertainty in the model output was studied through a series of experiments, whereby skewness was varied incrementally, and jointly for all parameters, within a fixed interval representing a tolerance of ±100% (CV = 37.8%) on the parameter mode. This was the maximum interval allowed without violation of parameter range constraints. It should be noted in passing that whilst skewness and uncertainty were addressed separately in this study, they are intrinsically linked, and a systematic change in skewness of a parameter distribution corresponds to a change in uncertainty in the parameter itself (in addition to the effect on model output uncertainty). This interesting behaviour is demonstrated by inspection of the effect of a change in skewness on the shape of the cumulative probability distribution of a parameter. In addition to skewness, the effect of kurtosis, which is a measure of the peakedness of a distribution, was also studied.

Skewness and kurtosis can be represented by dimensionless metrics, s_w and k_t, respectively, which are estimated from sample statistics $\bar{x}$ and s, using the following expressions for a discrete univariate series [16,14],

$$s_w = \frac{\sum_{i=1}^{i=n} (y_i - \bar{y})^3}{(n-1)s^3} \tag{6}$$

$$k_t = \frac{\sum_{i=1}^{i=n} (y_i - \bar{y})^4}{(n-1)s^4}. \tag{7}$$

The distribution is left-skewed (negative skewness values) if the tail is much longer on the left and is right-skewed (positive skewness values) if the tail is much longer on the right. The higher the kurtosis, the more peaked is the distribution.

2.5. Sensitivity analysis

Three types of sensitivity analysis were performed. The first two types were stochastic in nature and required a series of parameter conversions from distributions to fixed values, in successive simulations, and observation of the effect on the model output uncertainty metrics (90% CI and variance). The variance of the model output distribution depends on the variances of the parameter distributions — and if a parameter is converted to a constant value then its effect is removed from the model output variance. Starting with the full model, parameters were progressively held constant in a step-wise fashion (i.e. in a cumulative manner) for successive Monte Carlo simulations. The initial order of parameter fixing was β_2, β_3, ω, $HQ_{\max}$, $AQ_{\max}$, and this order was then reversed in a second experiment. This exercise enabled the relative influence of the various parameters on the model output uncertainty to be gauged, and provided a check for correlation.

The third sensitivity analysis involved plotting a deterministic sensitivity series for each parameter, analogous to a classical 'spider-plot'. From the base level vector, each parameter was varied incrementally while holding the remaining parameters constant. The percentage change in value for the parameter was plotted against the corresponding percentage change in value of the model output (streamflow). The five plots for the five parameters revealed the magnitude and sensitivity of the model output to small changes in parameter values.

The three previous analyses clearly identified that two parameters, β_3, and $AQ_{\max}$, had the greatest influence on both the uncertainty and magnitude of the model output (the details are described in the experimental section).

These parameters appear at one point in the model: the flux equation for the baseflow prediction, AQ (see Appendix, Eq. (A.8)), which relates to discharge from the alluvial store. The influence of these two parameters on the flux equation was studied in the third sensitivity analysis exercise. First, AQ was calculated over a range of β_3 values, with all other parameters being held constant. Second, the sensitivity of the output variance, $\sigma^2(AQ)$, as a function of β_3 was determined using differential analysis [17]. Differential error analysis theory states that if the x_i values are not correlated, the variance of the output can be calculated as

$$\sigma^2(y) \cong \sum_{i=1}^{n} \left[\frac{\partial f(\mathbf{x}_0)}{\partial x_i}\right]^2 \sigma^2(x_i). \tag{8}$$

Therefore, the variance of the output of the baseflow flux equation was calculated as

$$\sigma^2(AQ) = \sigma_1^2(AQ) + \sigma_2^2(AQ), \tag{9}$$

where the contributions from errors in $AQ_{\max}$ and β_3 (for an arbitrary time step, t), are given by

$$\sigma_1^2(AQ) = \left(\frac{AS}{AS_{\max}}\right)^{2\beta_3} \sigma^2(AQ_{\max}) \tag{10}$$

$$\sigma_2^2(AQ) = \left[AQ_{\max}\left(\frac{AS}{AS_{\max}}\right)^{\beta_3} \ln\left(\frac{AS}{AS_{\max}}\right)\right]^2 \sigma^2(\beta_3) \tag{11}$$

and the associated normalised errors, F_1 and F_2, are functions of β_3, i.e.

$$F_1 = \frac{\sigma_1^2(AQ)}{\sigma^2(AQ_{\max})} = \left(\frac{AS}{AS_{\max}}\right)^{2\beta_3} \tag{12}$$

$$F_2 = \frac{\sigma_2^2(AQ)}{\sigma^2(\beta_3)} = \left[AQ_{\max}\left(\frac{AS}{AS_{\max}}\right)^{\beta_3} \ln\left(\frac{AS}{AS_{\max}}\right)\right]^2. \tag{13}$$

2.6. Simulation procedure

The 2C model was coded in Visual Basic (VBA with Excel interface) and Monte Carlo simulations carried out using the software package @RISK, version 4.5.2 Professional Edition (Palisade Corporation, Newfield, New York). Sampling from input probability distributions was subject to the Latin Hypercube method, which executes stratified random sampling across the full range of each parameter without replacement [18,19]. The Latin Hypercube approach provides more uniform sampling in the tails than traditional random sampling in Monte Carlo simulation and generally leads to much faster convergence [12].

The number of iterations required to estimate a mean can be determined using standard sampling theory [16], and for the case of streamflow was found to be around 500, allowing for up to 1% error. However, when estimating variance and 90% CI of the output, a far greater number of iterations is typically required. Using the method described by Robinson [20] it was determined that the minimum number of iterations required to satisfy an error of $<1\%$ is about 20,000. Therefore, to be conservative 30,000 iterations were conducted for all simulations.

3. Results and discussion

Model predictions were quite tolerant to significant variation in parameter values. This is shown in Fig. 4, where it is evident that the 95th percentile predictions of the model for annual streamflow vary little in response to significant changes in the coefficient of variation (CV) for the five parameters (which were represented by symmetric probability density functions simulated by PERT distributions with zero skewness). For example, the 95th percentile result increased by less than 1.5%, despite an increase of the CV for the five parameters jointly from 7.6% to 37.8% (the latter representing an incremental change in tolerance from $\pm 20\%$ to $\pm 100\%$ about the mean of each parameter). That is, a significant change in the width of the parameter distribution resulted in only a small change in the 95th

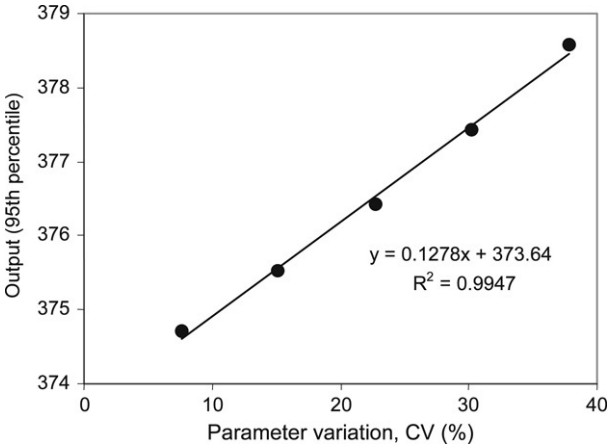

Fig. 4. Risk plot showing 95th percentile results for predicted annual streamflow (kL).

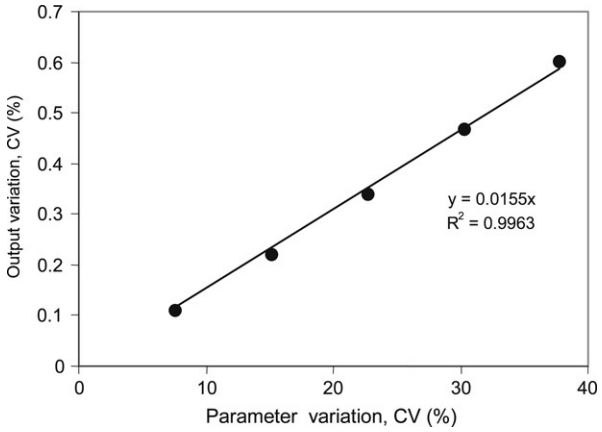

Fig. 5. The gain factor, G, is the slope (amplification) in model prediction error for streamflow due to a forced perturbation on the parameters.

percentile value of the output. This behaviour can also be appreciated through consideration of the gain factor, G, which is a measure of amplification or attenuation in the output due to changes in the parameters, and represents the slope of the plot in Fig. 5. In this case, for the prediction of streamflow, it is clear that a large change in the five parameters results in a relatively smaller change in model output ($G = 0.0155$). Inspection of the internal structure of the 2C model suggests that this behaviour is due to the compressive effect imposed by the non-linear flux equations, which are characterised by exponential models in which the base is fractional. The implication of this is that, since the parameters are derived by non-linear regression analysis using site measurements, the 2C model may not be very sensitive to errors or variability in calibration.

Increasing the joint variation in the parameter values reveals a correspondence with the output variance from the Monte Carlo simulation (Fig. 6). However, as the variability of the parameter distributions increases, so does the skewness and kurtosis of the output distribution, which suggests the variance is gradually becoming less effective as a characterisation of the output distribution and therefore uncertainty. Conversely, at low parameter variation, the output distribution skew and kurtosis (0 and 3, respectively) approximate a (symmetric) normal distribution. A direct proportional relationship between the CV of the parameters and the 90% CI of the output was observed (Fig. 7). The linear relationship is preserved even at the highest levels of parameter variability. This represents a consistent characterisation of output uncertainty in the presence of increasing skewness in the output distribution, unlike variance. Therefore, the 90% CI – when calculated from the cumulative probability distribution curve (difference between 5th and 95th percentile values) – is a more appropriate measure of output uncertainty in this model than is the variance.

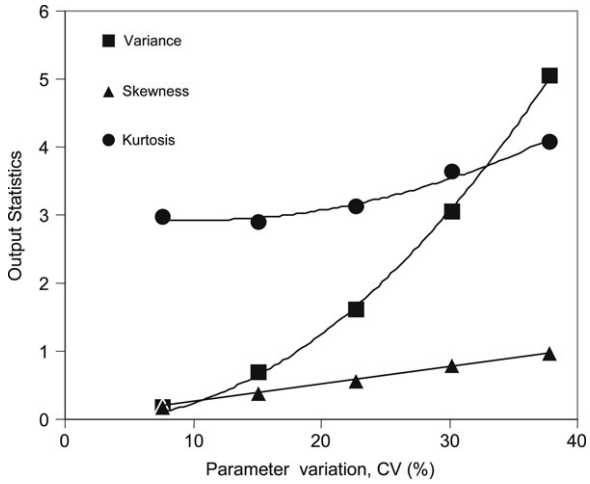

Fig. 6. Output distribution statistics as a function of increasing parameter variation.

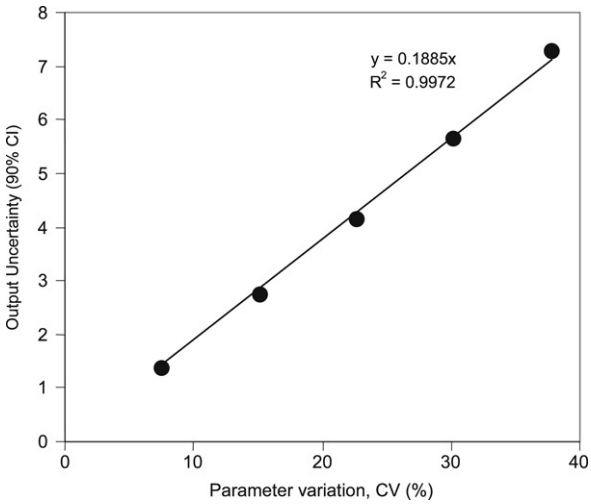

Fig. 7. Output uncertainty (90% CI) due to increasing parameter variation.

Fig. 8 shows a plot of two measures of uncertainty, namely 90% CI and variance of the output distribution, against skewness, s_w, of the parameter distributions. Maximum uncertainty occurs at a skewness value of $s_w \approx 0.55$ for the curve for 90% CI, but does not coincide with the maximum in the curve for variance (noting also the displacement between the curves at each end). This result suggests that using variance as an uncertainty measure in this case introduces a slight error. Also, the range in skewness in the parameter distribution can easily double the uncertainty in the output (90% CI). Fig. 9 shows a strong non-linear relationship between the skewness in the parameter distributions and the skewness in the output distribution. Therefore, if skewness of the parameter distribution will affect output uncertainty, then uncertainty is more accurately characterised by the CI rather than variance (which has implications for any variance-based sensitivity approaches, such as the computationally intensive MCMC — Global Sensitivity Analysis [9]).

It is clear from Fig. 10 that a significant drop in output uncertainty occurs when β_3 and then $AQ_{\max}$ were held constant in the Monte Carlo simulation. Progressive conversion of the remaining parameter distributions to constant (mean) values had negligible effect on output uncertainty. The influence of these two parameters was confirmed by reversing the order of parameter fixing (Fig. 11). In this case, a significant drop in output uncertainty occurred when first $AQ_{\max}$ and then β_3 are held constant. Inspection of the data reveals no hysteresis effect, i.e. the same pattern of change in uncertainty was repeated for the reverse series. These results also suggest that no significant interaction

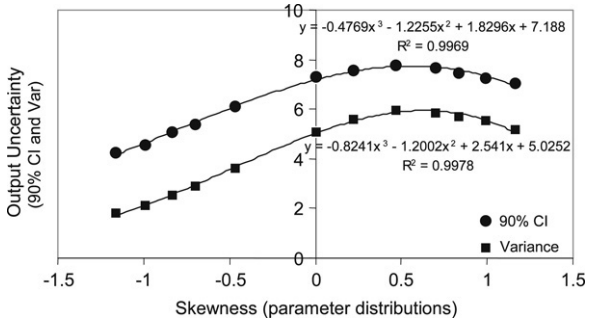

Fig. 8. Output uncertainty (90% CI and variance) as a function of skewness, s_w, of the parameter distributions.

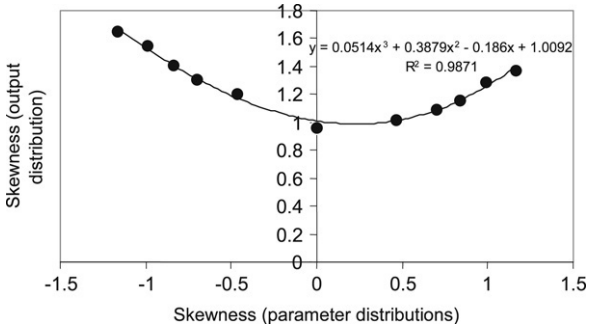

Fig. 9. Skewness of parameter distributions and its effect on skewness of output distribution.

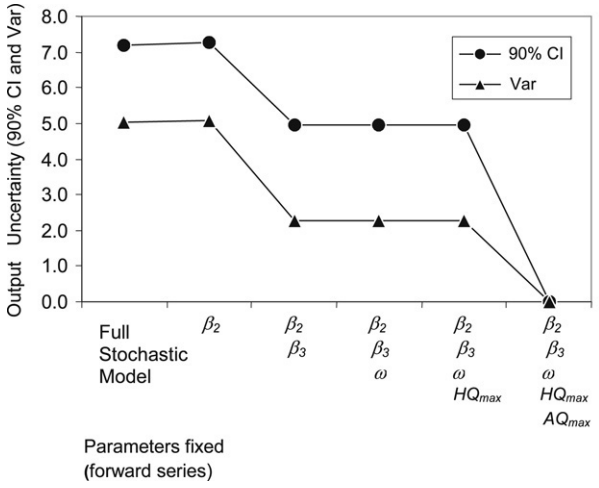

Fig. 10. Effect on uncertainty with successive simulations, where all five-parameter distributions are progressively replaced with their fixed (mean) values (forward series).

or correlation exists between the parameters. This result appears reasonable by inspection of the parameters in the mathematical structure of the model equation. The deterministic sensitivity analysis (Fig. 12), where each parameter was varied independently whilst holding the others constant, indicated that the change in predicted streamflow is relatively small (less than 1.5%), but due almost entirely to sensitivity to β_3 and $AQ_{\max}$ (with negative and possible correlations with output, respectively).

The importance of β_3 in the flux equation (Eq. (A.8) in Appendix) can be gauged from the plot in Fig. 13. The deterministic sensitivity of AQ to β_3 is clearly shown with the following trend evident,

$$\text{for } \beta_3 \geq 0.5, \quad \text{as } \beta_3 \to \infty, \quad \Delta AQ \to 0$$

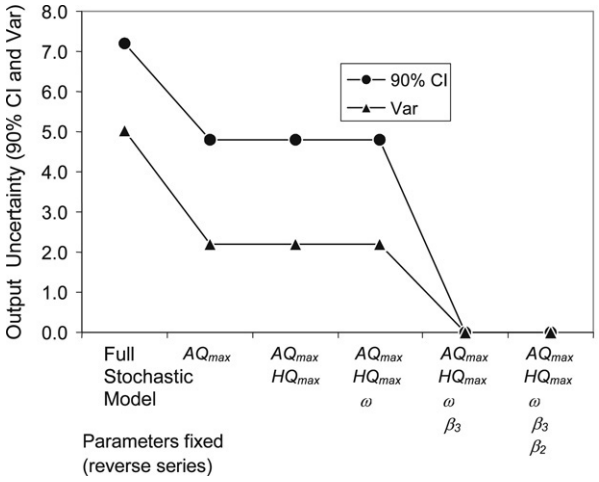

Fig. 11. As in Fig. 10, but with the process carried out in reverse order.

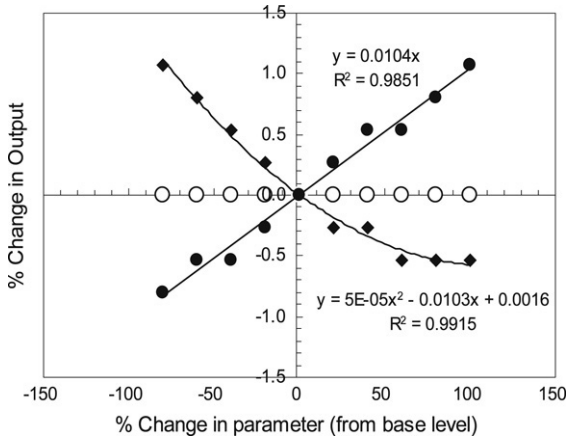

Fig. 12. Sensitivity series for five parameters for predicted annual streamflow (where ♦ $= \beta_3$, ● $= AQ_{\max}$, ○ $= \beta_2, \omega, HQ_{\max}$).

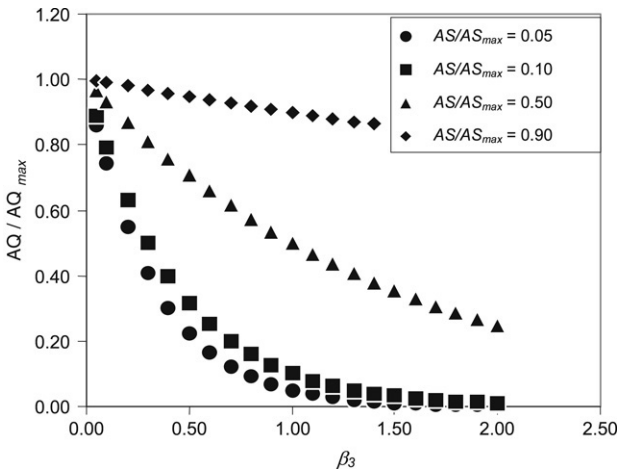

Fig. 13. Baseflow flux prediction ($AQ/AQ_{\max}$) as a function of β_3 (at base level, $AQ_{\max} = 10$).

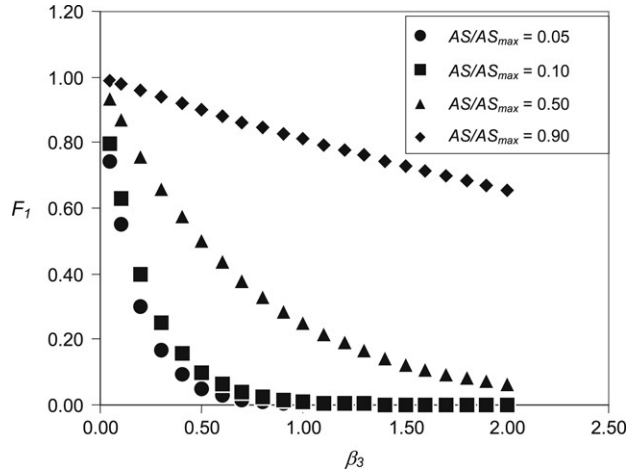

Fig. 14. Normalised variance of baseflow flux, F_1, as a function of β_3.

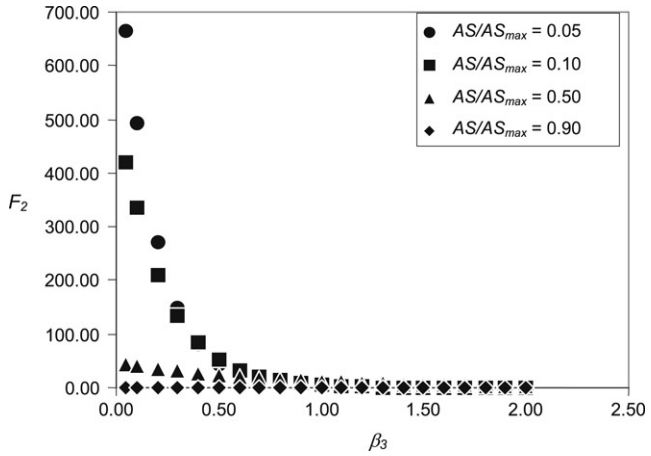

Fig. 15. Normalised variance of baseflow flux, F_2, as a function of β_3, for $AQ_{\max} = 10$.

$$\text{for } \beta_3 < 0.5, \quad \text{as } \beta_3 \to 0, \quad \Delta AQ \to AQ_{\max}. \tag{14}$$

In particular, for $\beta_3 \geq 1$, there is a much less dramatic change in the flux, AQ. That is, for a given calibration, if this parameter is around unity or above in magnitude then this over-sensitivity is less evident. Sensitivity is very acute below $\beta_3 = 0.5$ where only a small change in β_3 can result in a very large change in AQ. This behaviour should be taken in the context of calibration exercises, where the parameter often has a value near unity for the 2CSalt version of 2C in the case of the *Bet Bet* catchment [2].

The error in AQ due to errors in $AQ_{\max}$ and β_3 is plotted in Figs. 14 and 15, respectively. These plots reveal that the variance (uncertainty) in the output AQ is represented by a series of exponential decay models ($R^2 = 1.0$), and is highly dependent on the parameter β_3, irrespective of the ratio of $AS/AS_{\max}$. This trend is consistent with the expressions relating β_3 to the normalised error in baseflow flux, AQ, see Eqs. (12) and (13), and again indicates lower uncertainty in the output for $\beta_3 \geq 0.5$.

This last trend correlates with, and is supported by, the plot for uncertainty against skewness of the input parameter distribution (Fig. 8), which shows that peak uncertainty occurs at a value of $s_w \approx 0.55$, which is equivalent to a mean value for $\beta_3 = 0.60$ for the skewed PERT distribution. During the Monte Carlo simulation, input distributions with *positive* skewness produced low β_3 values close to the origin — therefore increasing output uncertainty, which again is consistent with the observations above. In summary, lower uncertainty in the output is associated with $\beta_3 \geq 0.5$, with particular improvement evident at a value of 1.0 or higher.

4. Conclusion

Uncertainty is inherent in the structure of a predictive model, in the input data, and in the model parameters due to calibration difficulty. The advantage of uncertainty analysis is that it provides methodologies that can add value to conventional risk analysis by providing more information about the outputs of a predictive model, and identifies components of the model where uncertainties can be decreased. For an analyst, model user, or policy maker, uncertainty analysis also has the advantage of providing an error bound and confidence level on the output. This investigation did not address the issue of parameter estimation itself but rather the impact of parameter uncertainty on model output uncertainty. The main objective was to study uncertainty methodology and uncertainty propagation with hydrology as the test application. Uncertainty was explored by various methods, including differential error analysis, Monte Carlo simulation and various forms of sensitivity analysis (based on computational simplicity and suitability for shape analysis of skewed distributions). The mathematical tools used are applicable to uncertainty analysis for water-balance or similar models [3–5] or predictive models in general.

It was clear that the model output uncertainty depended on the shape (skewness) of the parameter distributions, with increasing negative skewness leading to decreasing width of the output confidence interval (i.e. resulting in less uncertainty). Characterisation of uncertainty by variance was accurate for symmetrical distributions, but not for skewed distributions, where the preferred measure is the confidence interval from the cumulative distribution (e.g. for 90% CI, the difference between the 5th and 95th percentile values). The uncertainty analysis conducted here on the 2C hydrological model suggested that annual streamflow predictions are generally insensitive to substantial variation in the parameter values — i.e. variation greater than that likely to arise from calibration error. Sensitivity analyses identified two parameters, $AQ_{\max}$ and β_3, in the baseflow equation as having a dominant effect on model output uncertainty. A sensitivity series indicated that these parameters correlated negatively and positively with baseflow, respectively. Differential analysis revealed that the flux equation for baseflow, AQ, was very sensitive to β_3 — and values of β_3 greater than unity are associated with lower output uncertainty for AQ. The importance of this result is that AQ, or baseflow, is the dominant determinant of salt load prediction, which is a key application of the model.

The methods and findings reported here for the 2C hydrological model should prove useful for future applications with similar data inputs (noting that the parameters were perturbed in a systematic way and over a large range of values). The results are also consistent with a subjective observation by an author of a past study [2], suggesting the possible sensitivity of the model output to the parameter β_3. The approach described for uncertainty modelling provides a means to estimate the confidence interval for the output of the 2C model, which is more valuable to the model user than a single point estimate. A more demanding exercise would be the characterisation and propagation of uncertainty arising from both parameters and data inputs, a computationally very intensive study requiring very large data sets with both temporal and spatial variation possible. This is, however, a subject for future studies.

Acknowledgements

The authors are indebted to Craig Beverly and Brendan Christy at DPI Rutherglen for helpful discussions and insights with respect to hydrological modelling and water catchment analysis.

Appendix

The 2C model (version for streamflow prediction) comprises three stores: the unsaturated zone, the hillslope aquifer and alluvial mixing store. The equations below describe the balance of each store and show how streamflow is calculated [2,3]. The 2CSalt version of 2C contains thresholds in the flux equations, rather than in the constraints.

Symbols

Area	Area of Store 1, m^2
Area_{GRU}	Total area of GRU, including hillslope and alluvial stores, m^2
AlluvialArea	Area of alluvial store ($\text{Area}_{\text{GRU}} - \text{Area}$) m^2
R_t	Monthly hillslope recharge for all HRUs overlying GRU (spatially averaged) m^3
RO_t	Monthly hillslope runoff for all HRUs overlying GRU (spatially averaged) m^3
LF_t	Monthly hillslope lateral flow for all HRUs overlying GRU (spatially averaged) m^3

ASR_t	Monthly alluvial recharge for HRUs overlying alluvial store area, m^3
$ASRO_t$	Monthly alluvial runoff for HRUs overlying alluvial store area, m^3
$ASLF_t$	Monthly lateral flow for HRUs overlying alluvial store area, m^3
$Epot_t$	Monthly potential evaporation for HRUs overlying alluvial store area, m^3
EAS_t	Monthly evaporation from alluvial store area, m^3
HS_t	Storage of hillslope aquifer (store 2), m^3
HQ_t	Discharge from hillslope aquifer (store 2), m^3
AS_t	Storage of alluvial store, store 3, m^3
AQ_t	Discharge from alluvial store, store 3, m^3
Excess2	Overflow of water from store 2 assumed to go to stream, m^3
Excess3	Overflow of water from store 3, assumed to go to stream, m^3
β_2	Shape parameter for storage/discharge for store 2
β_3	Shape parameter for storage/discharge for store 3
ω	Shape parameter for evaporation from store 3
$HS_{\max}$	Maximum storage of hillslope aquifer, store 2, m^3
$HQ_{\max}$	Maximum discharge from hillslope aquifer, store 2, m^3
$AS_{\max}$	Maximum storage of alluvial store, store 3, m^3
$AQ_{\max}$	Maximum discharge from alluvial store, store 3, m^3

A.1. Unsaturated zone store

Spatial data files provide time series, with monthly time step, t, for recharge (R_t), lateral flow (LF_t) and runoff (RO_t), which are *spatially averaged* for all HRUs overlying the GRU (Fig. 2):

$$R_t = \sum_{i=1}^{\mathrm{HRU}} \frac{\mathrm{Hillslope\_Recharge}_{i,t} \times \mathrm{Area}_i}{\mathrm{Area}_{\mathrm{GRU}}}; \qquad LF_t = \sum_{i=1}^{\mathrm{HRU}} \frac{\mathrm{Hillslope\_Lateral}_{i,t} \times \mathrm{Area}_i}{\mathrm{Area}_{\mathrm{GRU}}};$$
$$RO_t = \sum_{i=1}^{\mathrm{HRU}} \frac{\mathrm{Hillslope\_Runoff}_{i,t} \times \mathrm{Area}_i}{\mathrm{Area}_{\mathrm{GRU}}}. \tag{A.1}$$

A.2. Hillslope aquifer store

The hillslope aquifer store is a simple balance of water and salt. Amounts of recharge water enter the aquifer on a monthly basis, mix thoroughly and are then released over a long period, depending on aquifer size and physical properties.

Calculate Discharge from store.

$$HQ_t = HQ_{\max}\left(\frac{HS_{t-1}}{HS_{\max}}\right)^{\beta_2}. \tag{A.2}$$

$$\text{If } HQ_t > HS_{t-1} + R_t \quad \text{then } HQ_t = HS_{t-1} + R_t. \tag{A.3}$$

Update storage volume by adding recharge and removing discharge.

$$HS_t = HS_{t-1} + R_t - HQ_t \quad 0 \le HS_t \le HS_{\max}. \tag{A.4}$$

Check for overflow of water from hillslope store, assumed to go to stream.

$$\mathrm{Excess2}_t = \begin{cases} HS_t - HS_{\max} & \text{if } HS_t > HS_{\max} \\ 0 & \text{otherwise.} \end{cases} \tag{A.5}$$

$$\text{If } HS_t > HS_{\max} \text{ then set } HS_t = HS_{\max}. \tag{A.6}$$

A.3. Alluvial mixing store

Recharge from HRUs overlying alluvial store (Fig. 2), and for AlluvialArea > 0 then,

$$Epot_t = \sum_{i=1}^{\mathrm{HRU}} \frac{\mathrm{Alluvial\_Evap}_{i,t} \times \mathrm{AlluvialArea}_i}{\mathrm{Area}_{\mathrm{GRU}}}; \qquad ASR_t = \sum_{i=1}^{\mathrm{HRU}} \frac{\mathrm{Alluvial\_Recharge}_{i,t} \times \mathrm{AlluvialArea}_i}{\mathrm{Area}_{\mathrm{GRU}}}$$

$$ASRO_t = \sum_{i=1}^{\mathrm{HRU}} \frac{\mathrm{Alluvial\_Runoff}_{i,t} \times \mathrm{AlluvialArea}_i}{\mathrm{Area}_{\mathrm{GRU}}};$$

$$ASLF_t = \sum_{i=1}^{\mathrm{HRU}} \frac{\mathrm{Alluvial\_Lateral}_{i,t} \times \mathrm{AlluvialArea}_i}{\mathrm{Area}_{\mathrm{GRU}}}. \tag{A.7}$$

Compute discharge from alluvial store (baseflow) and evaporation (m^3).

$$AQ_t = AQ_{\max} \left(\frac{AS_t}{AS_{\max}} \right)^{\beta_3} \tag{A.8}$$

$$EAS_t = Epot_t \left(\frac{AS_t}{AS_{\max}} \right)^{\omega}. \tag{A.9}$$

Check sufficient water credits to satisfy debits in store. Compute mass balance and update storage volume.

$$AS_t = AS_{t-1} - EAS_{t-1} + HQ_t - AQ_{t-1} + ASR_t\,. \tag{A.10}$$

Check for overflow of water from alluvial store, assumed to go to stream.

$$\mathrm{Excess3}_t = \begin{cases} AS_t - AS_{\max} & \text{if } AS_t > AS_{\max} \\ 0 & \text{otherwise.} \end{cases} \tag{A.11}$$

$$\text{If } AS_t > AS_{\max} \quad \text{then set } AS_t = AS_{\max}. \tag{A.12}$$

Compute monthly streamflow.

$$\mathrm{Streamflow}_t = \begin{cases} RO_t + LF_t + ASRO_t + ASLF_t + \mathrm{Excess2}_t + \mathrm{Excess3}_t + AQ_t, & \mathrm{AlluvialArea} > 0 \\ RO_t + LF_t + ASRO_t + ASLF_t + \mathrm{Excess2}_t + HQ_t, & \text{otherwise.} \end{cases} \tag{A.13}$$

References

[1] T. Wagener, H.V. Gupta, Model identification for hydrological forecasting under uncertainty, Stochastic Environmental Research and Risk Assessment 19 (2005) 378–387.

[2] C. Beverly, B. Christy, A. Weeks, Application of the 2CSalt model to the Bet Bet, Wild Duck, Gardner and Sugarloaf Catchments in Victoria, Department of Primary Industries Victoria, 2006.

[3] M. Littleboy, UserGuide_2CSalt, Rev 1.0, CRC for Catchment Hydrology, Australia. www.toolkit.net.au, 2005.

[4] M. Gilfedder, M. Stenson, G. Walker, W. Dawes, Impact of land-use change on water and salt export from upland areas: Using the BC2C model as a prioritisation tool, Presented at International Water Conference, Auckland, 2005.

[5] M.A. Bari, K.R.J. Smettem, A daily salt balance model for stream salinity generation processes following partial clearing from forest to pasture, Hydrology and Earth System Sciences 10 (2006) 519–534.

[6] J.J. Gourley, B.E. Vieux, A method for identifying sources of model uncertainty in rainfall–runoff simulations, Journal of Hydrology 327 (2006) 68–80.

[7] K.J. Beven, A.M. Binley, The future of distributed models: Model calibration and uncertainty in prediction, Hydrological Processes 6 (1992) 279–298.

[8] G. Kuczera, E. Parent, Monte Carlo assessment of parameter uncertainty in conceptual models: The metropolis algorithm, Journal of Hydrology 211 (1998) 69–85.

[9] A. Kanso, G. Chebbo, B. Tassin, Application of MCMC-GSA model calibration method to urban runoff quality modelling, Reliability Engineering and System Safety 91 (2006) 1398–1405.

[10] D. Kavetski, G. Kuczera, S.W. Franks, Bayesian analysis of input uncertainty in hydrological modelling: 1. Theory, Water Resources Journal 42 (2006) W03407; 1–9.

[11] D. Kavetski, G. Kuczera, S.W. Franks, Bayesian analysis of input uncertainty in hydrological modeling: 2. Application, Water Resources Research 42 (2006) W03408; 1–10.
[12] D. Vose, Risk Analysis, John Wiley & Sons, Chichester, England, 2000.
[13] RiskAMP, Structured Data, LLC, www.riskamp.com. 2005.
[14] C. Croarkin, P. Tobias (Eds), NIST/SEMATECH e-Handbook of Statistical Methods. http://www.itl.nist.gov/div898/handbook/, 2006.
[15] M.D. McKay, Evaluating Prediction Uncertainty, LA-12915-MS, Statistics Group, Los Alamos National Laboratory, NM (USA). Feb. 9, 1995.
[16] J.E. Freund, Mathematical Statistics, Prentice-Hall, 1998.
[17] J.C. Helton, Uncertainty and sensitivity analysis techniques for use in performance assessment for radioactive waste disposal, Reliability Engineering and System Safety 42 (1993) 327–367.
[18] M.D. McKay, W.J. Conover, R.J. Beckman, A comparison of three methods for selecting values of input variables in the analysis of output from a computer code, Technometrics 21 (1979) 239–245.
[19] R.L. Iman, W.J. Conover, A Modern Approach to Statistics, Wiley, New York, 1983.
[20] S. Robinson, Automated analysis of simulation output data, in: Proceedings of the 2005 Winter Simulation Conference, 2005.